

Understanding Different Inhibition Actions of Surfactants for Mild Steel Corrosion in Acid Solution

Reham H. Tammam^{1,*}, Amany M. Fekry¹, Mahmoud M. Saleh^{1,2,*}

¹Department of Chemistry, Faculty of Science, Cairo University, Giza, Egypt.

²Chemistry Department, College of Science, King Faisal University, Al-Hassa, Saudi Arabia

*E-mail: reham_tammam@yahoo.com, mahmoudsaleh90@yahoo.com.

Received: 10 October 2015 / Accepted: 19 October 2015 / Published: 1 January 2016

The inhibition actions of different surfactants for corrosion of mild steel were studied by electrochemical impedance spectroscopy and polarization measurements and weight loss. Cationic surfactant: cetylpyridinium bromide (CPBr), non-ionic surfactant: triton (TX-100) and anionic surfactant: dodecyl benzene sulphonate (DBS) in 1 M H₂SO₄. The order of the determined protection efficiency was found to be CPBr > TX-100 > DBS, due to the differences in the molecular structures of the three surfactants. The adsorption extent of CPBr was found to be higher than both TX-100 and DBS. A positive shift in the value of E_{pzc} in presence of the CPBr was attributed to the specific adsorption of the halide ion Br⁻ which facilitates the physical adsorption of the CP⁺ which is commenced by chemisorption of the pyridinium ring via its π -electrons with the surface Fe atom. Polarization curves and Weight loss measurements confirm the protection efficiency trends for the three surfactants.

Keywords: Mild Steel, Iron, Polarization, Acid Inhibition, Acid Corrosion.

1. INTRODUCTION

Surfactants have long been used as corrosion inhibitors for different metals in different corroding media. They have been used as corrosion inhibitors for many metals such as Al [1-3], Cu [4,5] and Ni [6]. Cationic surfactants [7,8], anionic surfactants [9,10] and non-ionic surfactants [11,12] have been used as corrosion inhibitors for iron and steels in both HCl and H₂SO₄ solutions. The choice of a surfactant as an inhibitor depends on the metal and the composition of the corroding medium. Surfactant imparts its inhibition action through adsorption at the metal/solution interface. Usually, the hydrophilic moiety of the surfactant adsorbs on the metal surface while the hydrophobic moiety extend

on the solution face. The extent and mode of adsorption depend on the type of interaction between the metal and the surfactant molecule. Chemical adsorption takes place through charge transfer between certain delocalized π -electrons of the molecule and the empty d-orbital of the iron surface atom. Physical adsorption takes place through Van der Waals forces or electrostatic attraction [13-15].

The increase in the number of carbon atoms in the hydrophobic part has its impacts on the inhibition efficiency of the surfactant [16]. Maximum protection efficiency was obtained at the critical micelle concentration of the surfactant. Usually, and in case of physical adsorption via electrostatic attraction, the potential of zero charge, E_{pzc} plays an important role in the extent of adsorption of definite organic inhibitor on the iron surface. The influence of the charge on the metal surface was discussed by Antropov [17]. A potential difference, φ between the free corrosion potential, E_{cor} and the potential of zero charge, E_{pzc} ($\varphi = E_{cor} - E_{pzc}$) was introduced [17]. When E_{cor} is more positive than E_{pzc} it means that the iron surface acquires a positive charge in specific corroding medium, i.e., $\varphi = +ve$ value. On the other hand, when E_{cor} is more negative than E_{pzc} it means a negative iron surface, i.e., $\varphi = -ve$ value. Adsorption of cationic species such as a cationic surfactant is favored if φ is a negative value. In the other hand, adsorption of negative species such as anionic surfactant is favored if φ is a positive value [18,19]. Chemisorption, on the other hand, involves charge transfer or charge sharing from the inhibitor molecule and the metal surface [18,19]. In this case the closeness of the chemisorbed molecule may be favored in case of the presence of physical adsorption prior to chemical adsorption. Change of the surface charge of the metal surface by synergism or coadsorption of anions may facilitate the chemical adsorption of organic species [20,21].

It is the purpose of the present study to compare the inhibition characteristics of different surfactants using electrochemical impedance measurements, polarization measurements and weight loss measurements. The potential of zero charge of iron in different media is measured to enable us to interpret the different behaviors. The data are analyzed to study the adsorption extents of the three surfactants. Discussion of the different performance and its relation to different molecular structures will be introduced.

2. EXPERIMENTAL

The iron sample had a chemical composition of 0.17% C, 0.61% Mn, 0.19% Si, 0.02 % Ni, 0.02% B, 0.06% P and the remaining iron. The used surfactants were cetylpyridinium bromide (CPBr), Triton (TX-100) and dodecylbenzene sulphonate (DBS). The surfactants were obtained from Aldrich and used as received. The molecular structures of the used surfactants are shown in Fig. 1. Stock solutions of the surfactants were prepared in 1.0 M H_2SO_4 and the desired concentrations were obtained by appropriate dilutions. Bidistilled water was used in preparation of the solutions. De-aeration of the solution for 30 min. was performed using N_2 gas before measurements. The temperature was adjusted to $30 \pm 0.2^\circ C$ using a water thermostat.

Electrochemical measurements were performed using an EG&G Princeton Applied Research Model 273A potentiostat/galvanostat and a lock-in amplifier (model 5210), operated with Corr-352 and EIS M398 electrochemical software. Electrochemical measurements were carried out in a

conventional three-electrode cell. The iron electrode was fitted into a glass tube of proper internal diameter by using epoxy resins.

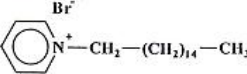
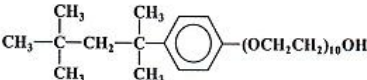
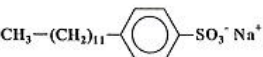
Surfactant	Chemical structure
Cetylpyridinium bromide (CPBr)	
Triton (TX-100)	
Dodecylbenzene Sulphonate (DBS)	

Figure 1. Molecular structures of the three inhibitors.

The exposed surface area of the electrode was 0.50 cm^2 . The iron electrode was polished gradually with emery paper down to 2000 grade. It was then washed with bidistilled water and finally degreased by rinsing with acetone and dried.

The counter electrode was made of a platinum sheet. The reference electrode was of the type $\text{Hg}/\text{Hg}_2\text{SO}_4/1\text{M H}_2\text{SO}_4$ with a Luggin probe positioned near the electrode surface. Note that the potential scale in the polarization curves was taken as the potential with respect to the NHE. The iron electrode was immersed for 30 minutes at the free corrosion potential, E_{cor} in the solution before the electrochemical measurements were recorded. Impedance (EIS) measurements were performed under free corrosion potential, whereas potentiodynamic polarization curves were recorded using potentiodynamic technique with a constant scan rate of 1 mV s^{-1} . The EIS measurements were carried out in the frequency range 10 mHz to 100 kHz and using a signal of amplitude 5 mV peak-to-peak. The measurements were repeated to test the reproducibility of the results. Weight loss measurements were achieved on circular iron discs of 1.8 cm diameter and thickness 0.5 cm. The iron disc was polished as mentioned above and immersed in 100 ml of the corroding solutions for 2 hour. The rate of corrosion for three similar iron discs in absence and presence of the surfactant was determined for each sample and the mean value was taken.

3. RESULTS AND DISCUSSION

3.1. Electrochemical experiments

3.1.1 Electrochemical Impedance Spectroscopy:

The measurements were achieved to determine the impedance parameters of the iron/electrolyte interface in presence of different concentrations of the inhibitors. Figures 2-4 show

the Nyquist plots of iron in absence and presence of the three surfactants (CPBr, TX-100 and DBS). In all cases, an increase of the inhibitor concentration causes an increase in the size of the semicircle indicating an increase of interface resistance. The increase in the semicircle size at specific concentration depends on the inhibitor. At low concentrations, the effect is not significant.

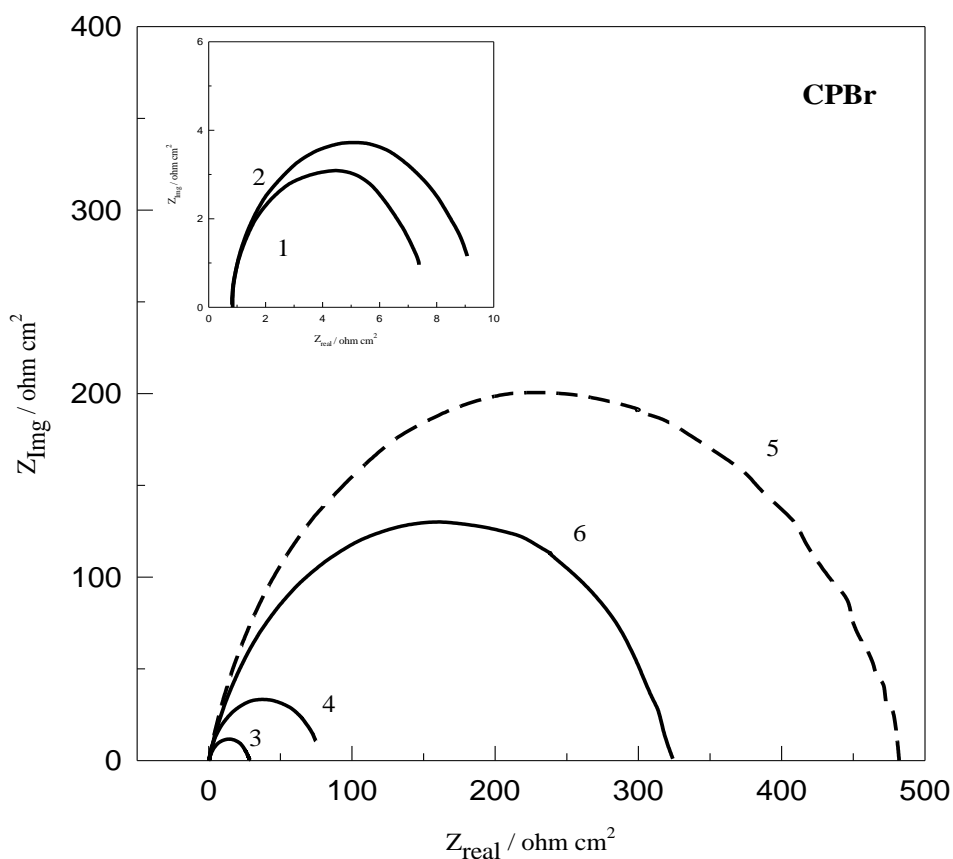


Figure 2. Nyquist plots of mild steel in presence of different concentration of CPBr. 1) blank, 1 M H₂SO₄ 2) 2×10^{-5} M 3) 5×10^{-5} M 4) 1×10^{-4} M 5) 5×10^{-4} M 6) 1×10^{-3} M CPBr in 1 M H₂SO₄.

Analysis of the experimental data of the EIS measurements using electrical equivalent circuits is generally performed to estimate the electrochemical parameters of interest for corrosion system. This was done by best fitting to a corresponding equivalent circuit that is corresponding to the EIS results as shown in Fig. 5. The equivalent circuit shows; R_s , CPE and R_p which represent the solution resistance, a constant phase element corresponding to the double layer capacitance and the polarization resistance (charge transfer resistance) associated with the corrosion process, respectively.

To present a satisfactory impedance simulation of the data in Fig. 2-4, it is important to replace the capacitor, C with a constant phase element (CPE) in the equivalent circuit (Fig. 5). This CPE is denoted as Q_{dl} in Table 1. This approach is well documented in literatures [22-24]. Generally, the use of CPE in modeling is to account for frequency dispersion behavior corresponding to some

physicochemical processes such as surface inhomogeneity resulting from surface roughness, distribution of the active sites, dislocations, impurities and adsorption of inhibitors [22-24].

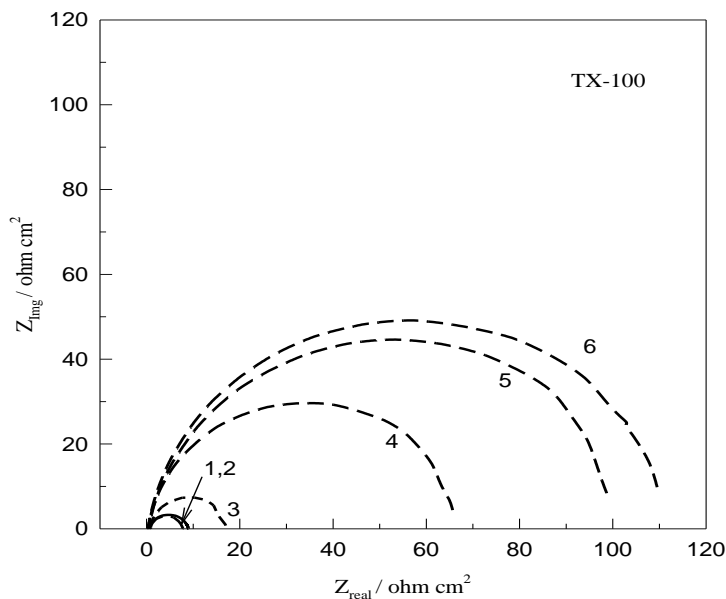


Figure 3. Nyquist plots of mild steel in presence of different concentration of TX-100. 1) blank, 1 M H₂SO₄ 2) 2×10⁻⁵ M 3) 5×10⁻⁵ M 4) 1×10⁻⁴ M 5) 5×10⁻⁴ M 6) 1×10⁻³ M TX-100 in 1 M H₂SO₄.

Table 1. Equivalent circuit parameters corresponding to EIS data in Figs. 2-4.

Electrode	C/ M	R _p / kΩ cm ²	Q _{dl} / μF cm ⁻²	R _s / Ω cm ²	α
Blank	0	7.69	207.3	0.52	0.78
CPBr	2×10 ⁻⁵	8.66	110.4	0.49	0.86
	5×10 ⁻⁵	28.0	95.1	0.49	0.85
	1×10 ⁻⁴	79.2	56.5	0.48	0.88
	5×10 ⁻⁴	460.3	22.9	0.48	0.91
	1×10 ⁻³	323.0	25.7	0.49	0.94
TX-100	2×10 ⁻⁵	8.31	115.0	0.53	0.86
	5×10 ⁻⁵	15.8	36.2	0.54	0.88
	1×10 ⁻⁴	63.0	54.9	0.50	0.85
	5×10 ⁻⁴	103.0	25.8	0.52	0.94
	1×10 ⁻³	110.7	24.0	0.53	0.91
DBS	2×10 ⁻⁵	8.27	151.0	0.47	0.76
	5×10 ⁻⁵	9.20	112.6	0.47	0.78
	1×10 ⁻⁴	19.0	83.5	0.46	0.75
	5×10 ⁻⁴	34.5	77.8	0.46	0.84
	1×10 ⁻³	39.5	62.2	0.47	0.81

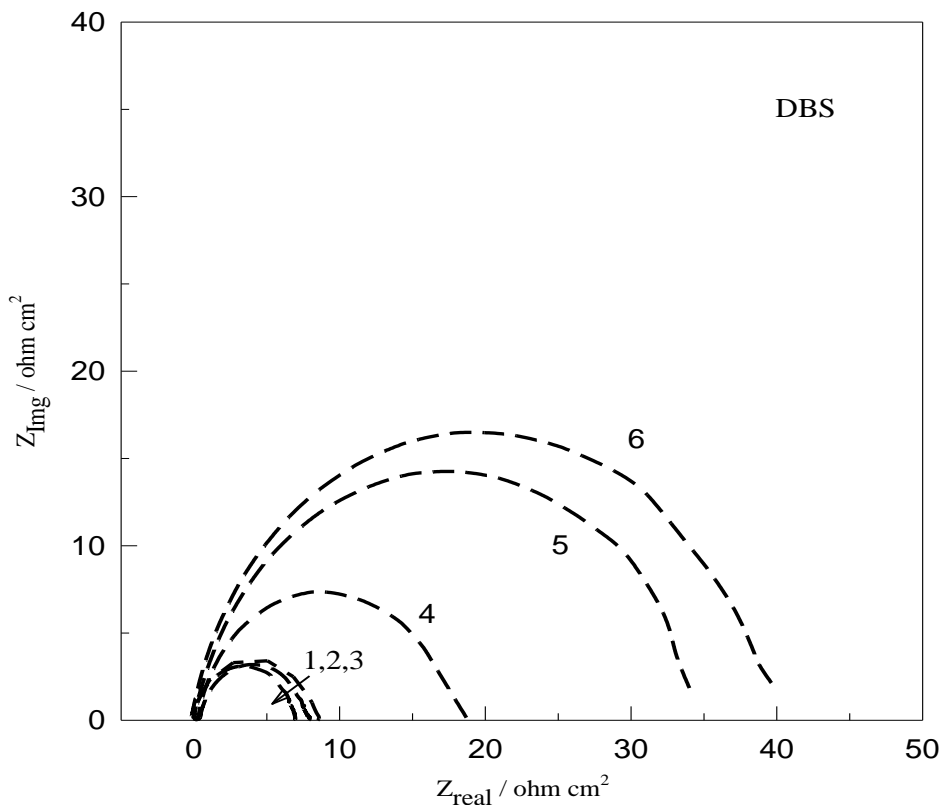


Figure 4. Nyquist plots of mild steel in presence of different concentration of DBS. 1) blank, 1 M H₂SO₄ 2) 2×10⁻⁵ M 3)5×10⁻⁵ M 4) 1×10⁻⁴ M 5) 5×10⁻⁴ M 6) 1×10⁻³ M DBS in 1 M H₂SO₄.

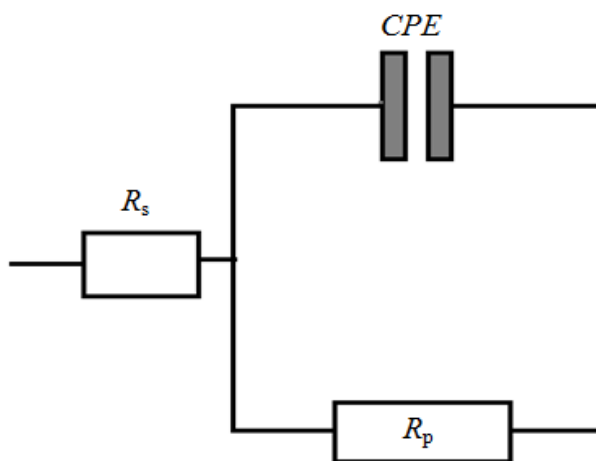


Figure 5. Equivalent circuit used to fit the data in Figs. 2-4.

The impedance (Z_{CPE}) of a constant phase element is defined as $Z_{CPE} = [C(j\omega)^\alpha]^{-1}$, where $-1 \leq \alpha \leq 1$, $j = (-1)^{1/2}$, $\omega = 2\pi f$ is the angular frequency in rad/s, f is the frequency in Hz = s⁻¹, α is a fitting parameter which is an empirical exponent varies between 1 for a perfect capacitor and 0 for a perfect

resistor. In this complex formula an empirical exponent (α) (see Table 1) varying between 0 and 1, is introduced to account for the deviation from the ideal capacitive behavior due to surface heterogeneity, roughness factor and adsorption effects [25,26]. In all cases, good agreement between theoretical and experimental data was obtained for the whole frequency range with an average error of 3%. The estimated parameters are given in Tables 1. The α values obtained from the fitting procedures are ranged between 0.75 and 0.94. This means that iron in absence and presence of the inhibitors does not behave as a perfect capacitor.

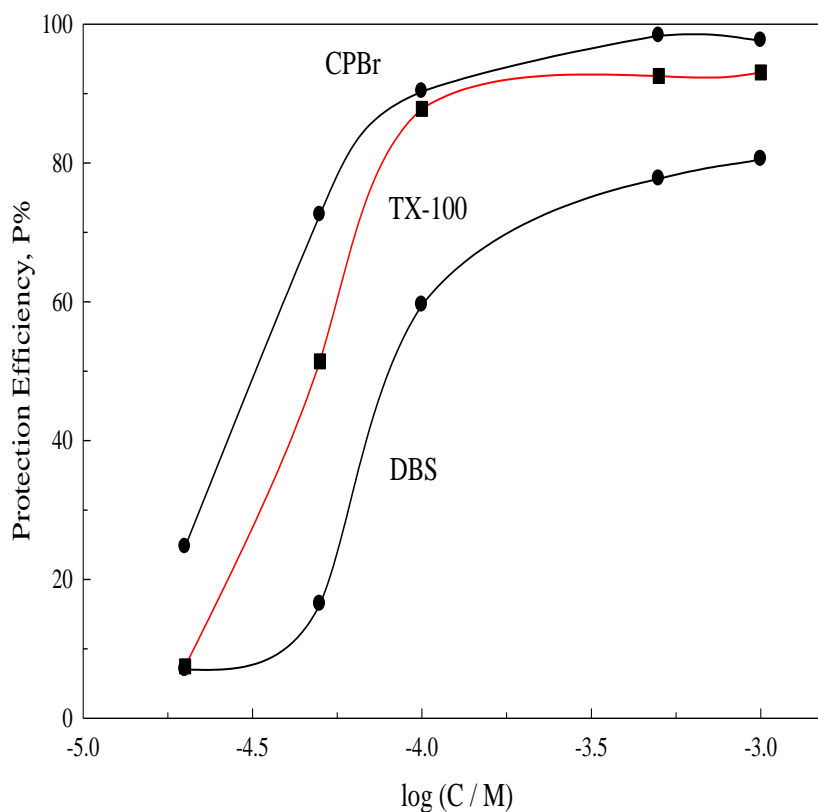


Figure 6. Protection Efficiency, P% of mild steel corrosion in presence of different surfactants.

For the anionic surfactant, DBS a significant increase of the semicircle size was obtained only at higher concentrations $\geq 1 \times 10^{-4}$ M. The cationic surfactant, CPBr showed the greatest effects (greatest increase in semicircle size) followed by TX-100 and then DBS. The increase of the semicircle size became insignificant at certain inhibitor concentration $\geq 5 \times 10^{-4}$ M. It is noteworthy to mention that the semicircle size in case of CPBr at concentration 1×10^{-3} M is smaller than that at concentration of 5×10^{-4} M. The double-layer capacitance, Q_{dl} is a measure of the exposed surface area or the corroding area and R_p is inversely proportional to the corrosion rate. For instance lower corrosion rates mean lower values of Q_{dl} and higher values of R_p . The presence of an efficient inhibitor usually decreases Q_{dl} and increases R_p . The evaluation of the values of R_p could be used to determine the protection efficiency of the inhibitor, as shown below.

The protection efficiency, %*P* represents a better way to quantify the effects of the different surfactants on the corrosion inhibition of the metals. The R_p values in absence and presence of different concentrations of the surfactants were used to determine the protection efficiency according to the following equation;

$$\%P = \left(1 - \frac{R_p(1)}{R_p(2)}\right) \times 100 \quad (2)$$

where $R_p(1)$ and $R_p(2)$ are the polarization resistances in absence and presence of the inhibitor. Figure 6 shows the protection efficiency of iron corrosion in presence of different concentrations of the surfactants at 30°C. As the concentration increases, the protection efficiency increases until it reaches constant values (plateau). The maximum values are dependent of the inhibitor. The plateau is corresponding to a concentration near the critical micelle concentration (CMC) of the surfactant. The reported values of the CMC were 8×10^{-4} , 4×10^{-4} and 1.0×10^{-3} M for CPBr, TX-100 and DBS, respectively [27,28]. They are all near 5×10^{-4} M. The cationic surfactant, CPBr shows the best protection efficiency followed by TX-100 and then DBS. At low concentration, the surfactant molecules replace the adsorbed water molecules on the iron surface. As the concentration increases more surfactant molecules replace water molecules leading to higher degree of surface coverage and hence to higher protection efficiencies. At concentration range higher than 5×10^{-5} M up to concentration before the plateau, the adsorption of the surfactant is supported by lateral interaction between the adsorbed molecules and hence leads to significant increase of %*P* through this range of concentrations [29]. At higher concentrations near the plateau, a bimolecular layer is possible [30]. At concentrations \geq CMC, the surfactant tends to form micelles rather than adsorbing on the iron surface leading to constant values of the protection efficiency. Note that in case of CPBr the %*P* at [CPBr] = 1×10^{-3} M is slightly smaller than that at [CPBr] = 5×10^{-4} M. This may be attributed to the adverse effects of the formation of an adsorbed bimolecular layer. In this case similar polar heads are directed towards the solution face with a possibility of repulsion between them. This was supported by the inclined molecular arrangement of the adsorbed CPBr molecules on the metal surface which has been previously suggested [31]. This may cause penetration of water molecules to the iron surface and hence weaker compactness of the surfactant layer.

3.1.2. Polarizations curves and weight loss:

The inhibition actions of the surfactants were also investigated by potentiodynamic polarization curves as shown in Figs. (7,8,9) for CPBr, TX-100 and DBS, respectively. The presence of the surfactant shifts the corrosion potential to more negative potential values. The shift depends on the surfactant and its concentration. The cathodic Tafel lines are shifted to lower currents or lower cathodic reaction rates. The anodic Tafel lines in case of the CPBr are shifted to lower currents but with much lower extents than that in the cathodic branches. The other two inhibitors have no effects on the anodic Tafel lines (Figs. 8,9). Generally, it may be concluded that the three surfactants act as cathodic inhibitors under the prevailing conditions. The shifts in cathodic lines are arranged as follows; CPBr > TX-100 > DBS.

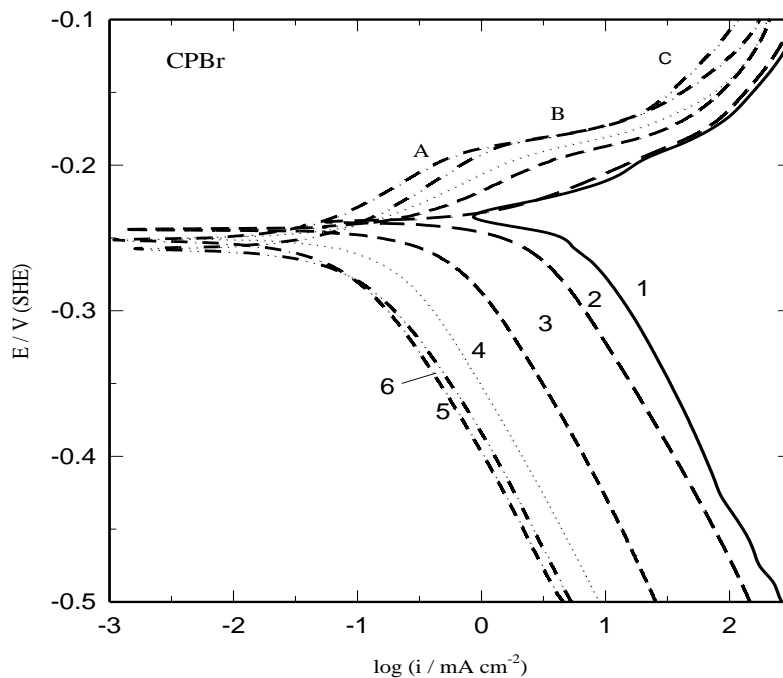


Figure 7. Polarization curves of mild steel in presence of different concentration of CPBr. 1) blank, 1 M H₂SO₄ 2) 2×10⁻⁵ M 3)5×10⁻⁵ M 4) 1×10⁻⁴ M 5) 5×10⁻⁴ M 6) 1×10⁻³ M CPBr in 1 M H₂SO₄.

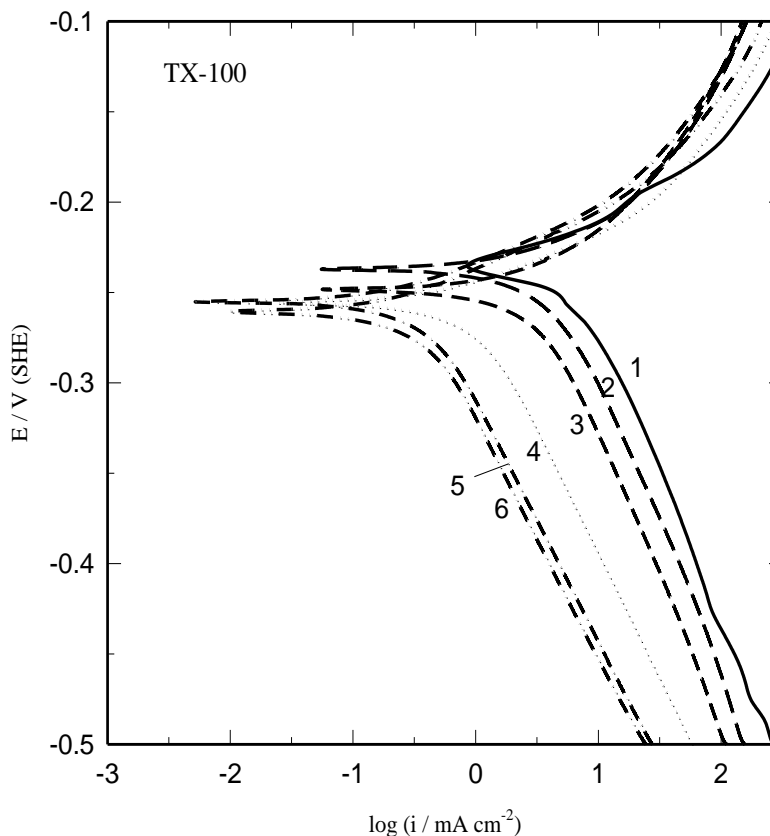


Figure 8. Polarization curves of mild steel in presence of different concentration of TX-100. 1) blank, 1 M H₂SO₄ 2) 2×10⁻⁵ M 3)5×10⁻⁵ M 4) 1×10⁻⁴ M 5) 5×10⁻⁴ M 6) 1×10⁻³ M TX-100 in 1 M H₂SO₄.

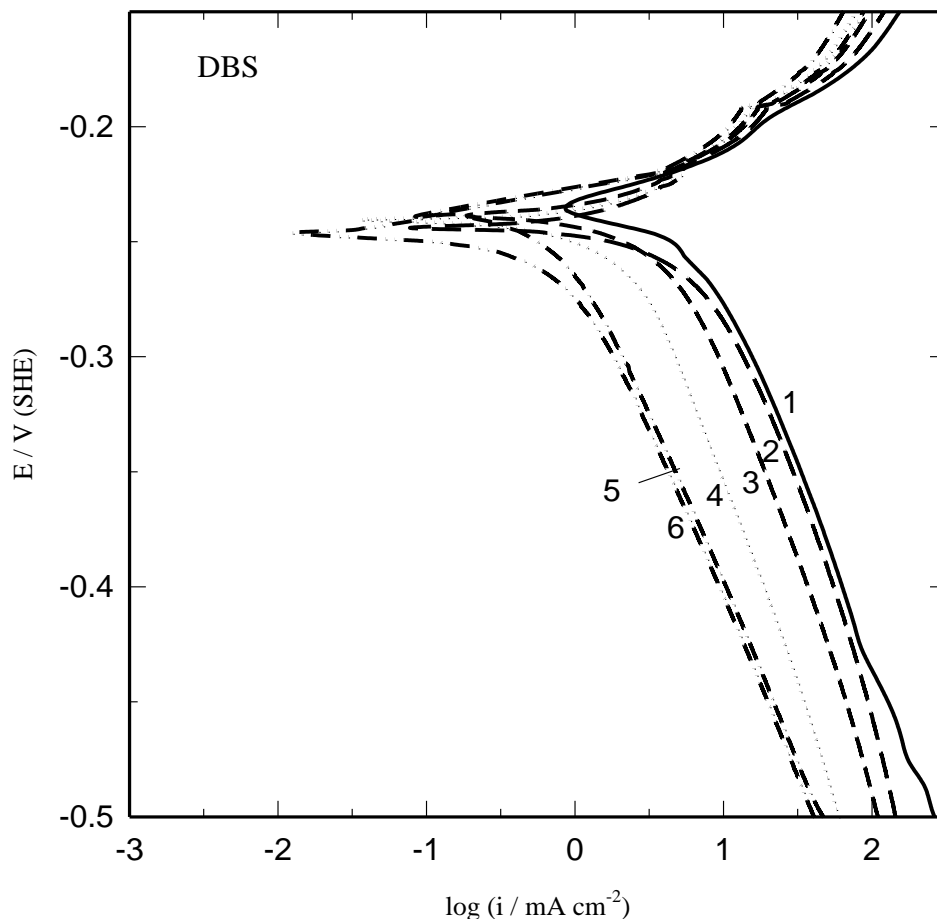


Figure 9. Polarization curves of mild steel in presence of different concentration of DBS. 1) blank, 1 M H_2SO_4 2) 2×10^{-5} M 3) 5×10^{-5} M 4) 1×10^{-4} M 5) 5×10^{-4} M 6) 1×10^{-3} M DBS in 1 M H_2SO_4 .

In case of CPBr we can recognize three regions in the anodic branches of the Tafel plots, mainly regions A, B and C, which represent the full inhibited region, flat and slightly inhibited regions, respectively. In region A, the CPBr shows inhibition action without any sign of desorption (inhibition region). At the start of region B and at a potential dependent of CPBr concentration the anodic curves begin to flatten (current increases) as a sign to the start of slight desorption of CPBr from the iron surface (flat region) [20]. In region C, moderate desorption (or higher extent of desorption) of the surfactant molecules take place with an extent dependent off the CPBr concentration [21]. Note that the other surfactants do not show such anodic behavior.

The electrochemical parameters of mild steel in presence of the different inhibitors are listed in Table 2. These include the free corrosion potential, E_{cor} , corrosion current density, i_{cor} , cathodic Tafel slope, B_c anodic Tafel slope, B_a and protection efficiency, $\%P_{\text{icor}}$. The slopes of the cathodic and anodic Tafel lines in presence of the inhibitors are comparable with that of the blank. The slopes of the cathodic Tafel lines in presence of the inhibitors are comparable with that of the blank. It indicates that the mechanism of the cathodic reaction does not change in presence of the inhibitor and the inhibition action is by simple blocking of the metal surface. The protection efficiency, $\%P_{\text{icor}}$ was determined

from the corrosion currents, i_{cor} in presence of different concentrations of the three surfactants. It can be calculated from i_{cor} values according to the following equation;

$$\%P_{icor} = \left(\frac{i_{cor1} - i_{cor2}}{i_{cor1}} \right) \times 100 \quad (3)$$

where i_{cor2} and i_{cor1} are the corrosion current densities in presence and absence of the inhibitor, respectively. The values of $\%P_{icor}$ are comparable with those extracted from the impedance data. Note that the value of $\%P_{icor}$ in presence of 1×10^{-3} M CPBr is slightly lower than that at 5×10^{-4} M in accordance with the impedance results.

Table 2. Electrochemical parameters derived from polarization curves.

Surfactant	C/M	E_{cor}/V (NHE)	$i_{cor}/mA\ cm^{-2}$	$B_c/mV\ dec^{-1}$	$B_a/mV\ dec^{-1}$	$\%P_{icor}$
CPBr	Blank	-0.2331	4.5	155	171	-
	2×10^{-5}	-0.2388	3.8	141	168	15.0
	5×10^{-5}	-0.2441	1.4	136	145	69
	1×10^{-4}	-0.2496	0.5	129	152	88
	5×10^{-4}	-0.2513	0.11	116	141	97.5
	1×10^{-3}	-0.2574	0.12	126	137	97
TX-100	2×10^{-5}	-0.2370	3.9	165	151	13
	5×10^{-5}	-0.2486	2.4	171	148	46
	1×10^{-4}	-0.2556	1.2	152	146	73
	5×10^{-4}	-0.2550	0.31	150	162	93
	1×10^{-3}	-0.2607	0.28	148	151	93.5
DBS	2×10^{-5}	-0.2439	4.2	173	160	6.7
	5×10^{-5}	-0.2383	3.98	170	164	11
	1×10^{-4}	-0.2406	1.78	165	154	60
	5×10^{-4}	-0.2349	0.79	145	151	82
	1×10^{-3}	-0.2478	0.79	147	143	82

The protection efficiency, $\%P_w$ was also determined by using the rates of corrosion data obtained from the weight loss measurements. It could be written as:

$$\%P_w = 100 \times \left(\frac{R_o - R_{inh}}{R_o} \right) \quad (4)$$

where R_{inh} and R_o are the corrosion rates in presence and absence of the inhibitor, respectively. The results are shown in Table 3. The values of $\%P_w$ (listed in Table 3) are in a satisfied agreement with the values obtained from both impedance and polarization measurements. The weight loss results confirm the above obtainable trends for the three surfactants.

Table 3. Rate of corrosion and protection efficiency from weight loss measurements.

Surfactant	C/M	Rate/ $mg\ h^{-1}\ cm^{-2}$	%P _w
CPBr	Blank, 1M	4.9	-
	2×10^{-5}	4.2	15
	5×10^{-5}	1.4	72
	1×10^{-4}	0.69	86
	5×10^{-4}	0.15	97
	1×10^{-3}	0.15	97
TX-100	2×10^{-5}	4.3	13
	5×10^{-5}	2.7	45
	1×10^{-4}	1.2	75
	5×10^{-4}	0.32	93.5
	1×10^{-3}	0.29	94
DBS	2×10^{-5}	4.5	8
	5×10^{-5}	4.2	14
	1×10^{-4}	2.1	75
	5×10^{-4}	0.96	80.5
	1×10^{-3}	0.93	81

3.2. Adsorption isotherm:

The degree of surface coverage, θ of the metal surface was calculated using the polarization curves and applying the following relation at constant potential, [32]

$$\theta = \left(\frac{i_1 - i_2}{i_1} \right) \tag{5}$$

where i_1 and i_2 are the current densities in absence (blank) and presence of surfactant, respectively at specific anodic potential of -0.4 V. This equation is valid under the condition of equal slopes of Tafel lines, a condition which is evident in the present cathodic Tafel lines. The values of θ were obtained for the different surfactants at different concentrations. The data of the surface coverage were found to fit with Langmuir isotherm which is given by:

$$\frac{\theta}{1 - \theta} = KC \tag{6}$$

where

$$K = \frac{1}{55.5} \exp \left(- \frac{\Delta G_{ads}^o}{RT} \right) \tag{7}$$

where C is the concentration of the inhibitor in the bulk of the solution, ΔG_{ads}^o is the free energy of adsorption. Figure 10 A-C show plots of Langmuir isotherms for the three inhibitors.

Satisfactory straight lines were obtained with slopes equal 1.0 ± 0.05 for the three surfactants. The free energy of adsorption, were determined from the intercepts of the plots in Fig. 10.

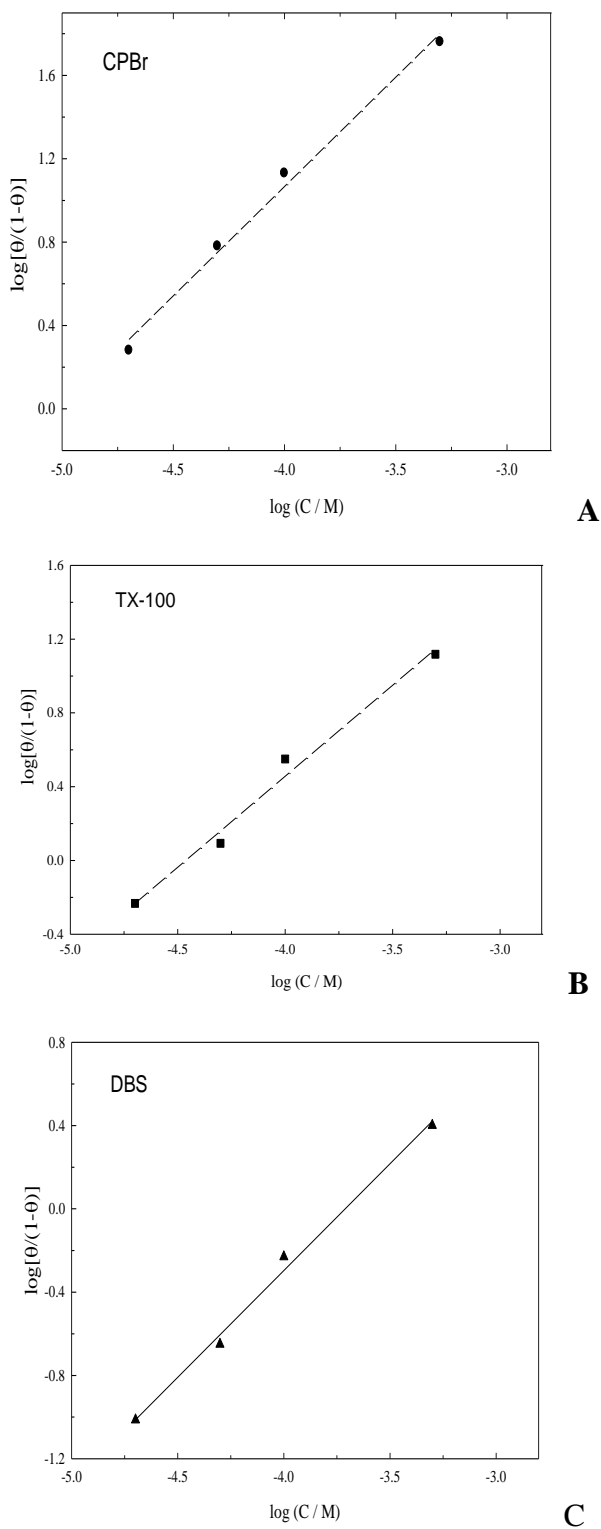


Figure 10. Langmuir isotherm for the adsorption of the three surfactants on mild steel at 30°C. A) CPBr, B) TX-100 and C) DBS.

The value of ΔG_{ads}^o was estimated to be -41.0, -34.0 and -32.0 kJ mol⁻¹ for CPBr, TX-100 and DBS, respectively. The above values may suggest chemisorption of CPBr and physisorption of TX-100 and DBS. In the other hand, CPBr shows higher adsorption affinity on the iron surface which is in accordance with the trends of the protection efficiency shown in Fig. 6.

3.3. Potential of Zero Charge:

In general it can be seen that the adsorption is affected by the nature of the surface charge on the corroded metal and by the molecular structure of the adsorbed organic compound. The immersion of the metal on a corroding solution results in the charge on the metal surface which is attributed to the electrical field which emerges at the interface. It can be determined using Antropov approach [17], by comparing the potential of zero charge, E_{pzc} and the corrosion potential of the metal in the electrolytic solution. Since E_{pzc} corresponds to a state at which the surface is free from charges, at the corrosion potential the metal surface will be positively or negatively charged. Accordingly it is important to measure the values of E_{pzc} in presence and absence of the inhibitors.

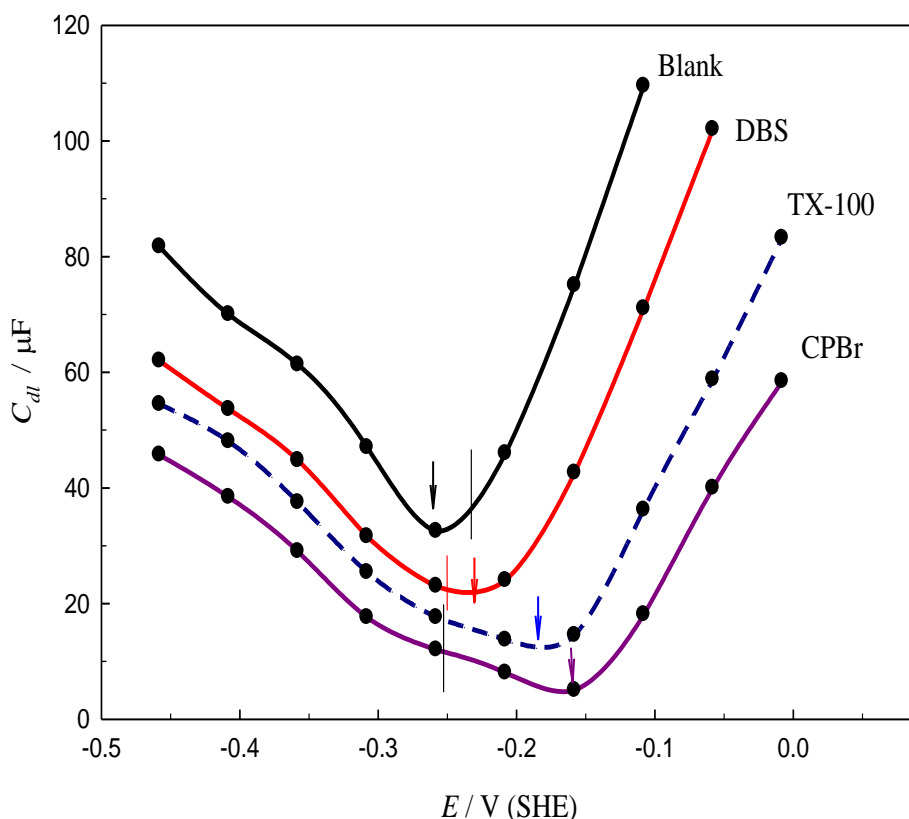


Figure 11. Variation of capacitance C_{dl} with potential E measured in 1 M H_2SO_4 (blank) and in 1 M H_2SO_4 containing 1×10^{-4} M CPBr, TX-100 and DBS.

Figure 11 depicts the variation of the capacitance, C_{dl} with the potential, E , measured in blank and in the presence of 1×10^{-4} M of the three surfactants. The figure shows V-shaped curve either in blank or in presence of the different surfactants. The minimum shown in the figure (pointed by an arrow) in each curve is assigned to the potential of zero charge, E_{pzc} . The drawn vertical line in each curve refers to E_{cor} in the corresponding solution. Table 4 lists the values of E_{cor} , E_{pzc} and ϕ . The value of ϕ in blank points to the fact that the iron surface is positively charged in the blank solution. This does not support the strong adsorption of CPBr cation (CP^+) on the iron surface. However, as shown in Table 4, the value of $\phi(CPBr) \approx -0.10$ V which demonstrates that the iron surface is negatively charged. This can be interpreted by specific adsorption of Br^- ions which modifies the charge of the iron/solution interface. This may interpret the high inhibition efficiency of the CPBr.

Since the value of the corrosion potential, E_{cor} in blank (1M H_2SO_4) is -0.2331 V (NHE) (see Table 4) and the $E_{pzc} = -0.2580$ V (NHE) and hence $\phi = E_{cor} - E_{pzc} = + 0.025$ V, and yet the iron surface is positively charged under these conditions. This result is in agreement with the literatures [16, 33]. In case of CPBr, the pre-adsorption of the Br^- ions on the positively charged metal surface may be the first step on the adsorption of the CPBr molecule [20].

Table 4. Values of E_{cor} , E_{pzc} and ϕ for mild steel in blank (1M H_2SO_4) and in presence of 1×10^{-4} M of CPBr, TX-100 and DBS.

Solution	E_{cor}/V	E_{pzc}/V	ϕ/V
blank	-0.2331	-0.2580	0.0249
CPBr	-0.2496	-0.1570	-0.0926
TX-100	-0.2556	-0.1838	-0.0718
DBS	-0.2406	-0.2210	-0.0196

The large negative value of ΔG_{ads}^o indicates chemical adsorption of CPBr due to presence of the pyridinium ring. That is to say, physical adsorption is first takes place and then chemisorption commences. Charge transfer between the π -electrons of the pyridinium ring and the empty d -orbital of the Fe atoms is considered. The adsorption of the CPBr molecule can be enhanced by the electrostatic attraction between the cation CP^+ and the induced negative sites resulting from the adsorption of the Br^- ion on the iron surface. The presence of the Br^- modifies the surface charge of the iron surface in a well-known process called synergism [16,20, 34,35].

In case of DBS and under the prevailing conditions one may expect strong adsorption of the negatively charge DBS anion. However, the opposite was found and DBS found to be less efficient than the other surfactants. This was attributed to the weak polarizability of the sulphonate group, $-SO_3^-$ [36]. In the other hand, TX-100 molecule has a slightly polar hydrophilic head composed of $(-OCH_2CH_2)_{10}OH$ moiety and a hydrophobic chain of (t-octyl-ph) group [37]. The values of $\phi \approx -0.07$ V (in case of TX-100) and yet the iron surface is slightly negative. TX-100 probably interacts with the charged iron surface via its hydrophilic moiety while the chain is directed towards the medium away from the surface. TX-100 gave lower efficiency than CPBr may be because the alkyl group (t-octyl-ph) in the molecule may take certain orientation to minimize the steric effects of such bulky group [4].

4. CONCLUSIONS

By an aid of the potential of zero charge, E_{pzc} , it has been possible to discuss the different inhibition actions of three surfactants; cetylpyridinium bromide (CPBr), triton (TX-100) and dodecyl benzene sulphonate (DBS) for mild steel in 1 M H_2SO_4 . Impedance, polarization and weight loss measurements were used to investigate the inhibition actions of the surfactants. The surfactants shifted the R_p value to higher values and also shifted the double layer capacitance of the iron/solution interface to lower values. Impedance and electrochemical showed that CPBr had the best inhibition action among the three surfactants. The three surfactants act mainly as cathodic inhibitors. The different actions were illustrated on the light of the different molecular structures of the inhibitors. Where CPBr gave best inhibition action, DBS suffered from the lower polarizability of the $-SO_3^-$ group and TX-100 gave lower inhibition actions due to presence of a bulky group. Specific adsorption of the halide ion, Br^- followed by physisorption via CP^+ and then chemical adsorption via pyridinium ring supported high inhibition efficiency of the CPBr compared to TX-100 and DBS.

References

1. V. Branzoi, F. Golgovici and F. Branzoi, *Mat. Chem. Phys.*, 78 (2002) 122
2. T. Zhao and G. Mu, *Corros. Sci.*, 41 (1999) 1937
3. E.E. Abd El Aal, S. Abd El Wanees, A. Farouk and S.M. Abd El Haleem. *Corros. Sci.*, 68 (2013) 14
4. A.K. Maayta, M.B. Bitar and M.M. Al-Abdalah, *Brit. Corr. J.*, 36 (2001) 133
5. R.F.V. Villamil, P.J. Corio, C. Rubin and S.M.L. Agostinho, *J Electroanal. Chem.*, 472 (1999) 112
6. R. Guo, T. Liu and X. Wei, *Journal of Colloid and Interface Science*, 289 (2005) 184
7. Lin-Guang Qiu, An-Jian Xie and Yu-Hua She, *Appl Surf Sci.*, 246 (2005) 1
8. R. Driver and R. J. Meakins, *Br. Corr. J.*, 12 (1977) 46
9. M. Hosseini, S.F.L. Mertens and M. R. Arhadi, *Corr. Sci.*, 45(2003) 1473
10. Mu G N, Zhao T P, Liu M and Gu T, *Corrosion*, 52 (1996) 853
11. M. Elachouri, M.S. Hajji, M. Salem, S. Kertit, J. Aride, R. Coudert and E. Essassi, *Corrosion*, 52(1996) 103
12. M.M. Osman and M.N. Shalaby, *Anti-Corr. Meth. Mat.*, 44 (1997) 318
13. V.S. Sastri, *Corrosion Inhibitors: Principles and Applications*, 1st Edn, John Wiley & Sons Ltd. New York (1998)
14. F. Bentiss, M. Traisnel and M. Lagrenee, *J Appl Electrochem.*, 31 (2001) 41
15. N. Hajjaji, I. Rico, A. Srhiri, A. Lattes, M. Soufiaoui and A. B. Bachir, *Corrosion*, 49 (1993) 326
16. D.P. Schweinsberg, V. Ashworth, *Corr. Sci.*, 28 (1988) 539
17. L.I. Antropov, *Inhibitors of Metallic Corrosion and the f-Scale of Potentials*, 1st Int. Cong. Metallic Corrosion (London, U.K Butterworths) p. 147(1962)
18. G. Banerjee and S.N. Malhotra, *Corrosion*, 48 (1992) 10
19. H. Luo, Y. C. Guan and K.N. Han, *Corrosion*, 54 (1998) 619
20. A. Khamis, M.M. Saleh and M.I. Awad, *Corr. Sci.*, 66 (2013) 343
21. A. Khamis, M.M. Saleh, M. I. Awad and B.E. El-Anadouli, *Corr. Sci.*, 74 (2013) 83
22. A.M. Fekry, *Electrochim Acta*, 54 (2009) 3480
23. D.D. Macdonald, *Electrochim Acta*, 51 (2006) 1376
24. A.M. Fekry, *Int. J. Hydrogen Energy*, 35 (2010) 12945

25. O. Olivares-Xometl, N.V. Likhanova, R. Martinez-Palou and M.A. Dominguez-Aguilar, *Mater. Corros.*, 60 (2009) 14
26. J.R. Macdonald, *J. Electroanal. Chem.*, 223 (1987) 25
27. M.M. Saleh and A.A. Atia, *J. Adsorption Science and Technology, Ads Sci Technol.*, 17 (1999) 53
28. D. Myer, *Surfactants Science and Technology*, VCH, New York(1988)
29. A. Frignani and F. Zucchi Monticelli, *Br. Corr. J.*, 18 (1983)19
30. M. Elachouri, M.S. Hajji, S. Kertit, E.M. Essassi, M. Salem and R. Coudert, *Corr. Sci.*, 37 (1995) 381
31. A.A. Atia and M.M. Saleh, *J. Appl. Electrochem.*, 33 (2003)171
32. B.G. Ateya, B.E. El-Anadouli and F.M. El-Nizamy, *Corr. Sci.*, 24 (1984) 509
33. A. Popova, E. Sokolova, S. Raicheva and M. Christov, *Corr. Sci.*, 45 (2003) 33
34. L. Larabi, Y. Harek, M. Traisnel and A. Mansri, *J Appl Electrochem* 34 (2004) 833
35. R. Chami, F. Bensajjay, S. Alehyen, M. El Achouri, A. Bellaouchou and A. Guenbour, *Colloids and Surfaces A: Physicochemical and Engineering Aspects* 480(2015)468
36. C. Monticelli, G. Brunoro, A. Frignani and F. Zucchi, *Corr. Sci.*, 32 (1991) 693
37. M.J. Schick. *Non-ionic Surfactants*, Marcel Dekker, New York(1987)

© 2016 The Authors. Published by ESG (www.electrochemsci.org). This article is an open access article distributed under the terms and conditions of the Creative Commons Attribution license (<http://creativecommons.org/licenses/by/4.0/>).